ISSN 0023-1584, Kinetics and Catalysis, 2008, Vol. 49, No. 2, pp. 202–211. © MAIK "Nauka/Interperiodica" (Russia), 2008.
Original Russian Text © S.L. Khursan, D.G. Semes'ko, A.N. Teregulova, R.L. Safiullin, 2008, published in Kinetika i Kataliz, 2008, Vol. 49, No. 2, pp. 214–223.

Analysis of the Reactivities of Organic Compounds in Hydrogen Atom Abstraction from Their C–H Bonds by the Sulfate Radical Anion $SO_4^{\bullet-}$

S. L. Khursan[a], D. G. Semes'ko[a], A. N. Teregulova[b], and R. L. Safiullin[b]

[a] *Bashkortostan State University, Ufa, 450074 Bashkortostan, Russia*

[b] *Institute of Organic Chemistry, Ufa Scientific Center, Russian Academy of Sciences, Ufa, 450054 Bashkortostan, Russia*

e-mail: Khursansl@gmail.com

Received November 8, 2006

Abstract—An experimental rate constant data array (>50 values) for the reactions of the sulfate radical anion with the C–H bonds of various organic compounds is analyzed by Denisov's intersecting parabolas method. The data array is divided into the following four groups according to the type of the C–H bond attacked and the br_e value: compounds with primary C–H bonds (br_e = 13.14 ± 0.17), compounds with secondary C–H bonds remote from the polar groups (br_e = 12.64 ± 0.34), compounds with secondary α-C–H bonds (br_e = 13.28 ± 0.24), and compounds with tertiary C–H bonds. It is demonstrated by DFT calculations that the rate constant of the reaction $SO_4^{\bullet-}$ + RH is determined by nonspecific solvation and by the ion–dipole interaction in the transition state of the reaction.

DOI: 10.1134/S0023158408020067

Salts of peroxydisulfuric acid, $A_2S_2O_8$ (A = K, Na, NH_4), are widely used as water-soluble initiators of free-radical chain processes [1]. Free radicals in this case are provided by the homolytic cleavage of the peroxide bond in the peroxydisulfate dianion $S_2O_8^{2-}$:

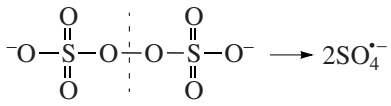

The $S_2O_8^{2-}$ dianion can decompose via thermal [2], photochemical [3], and radiation-induced [4] mechanisms. The resulting sulfate radical anion (SRA) propagates the homolytic reaction chain by reacting with an organic molecule. The reactions of SRA with organic compounds of various classes have been investigated in sufficient detail [5]. The following three basic mechanisms are possible for these reactions:

one-electron oxidation,

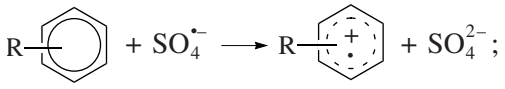

addition to a multiple bond,

$$H_2C{=}CHR + SO_4^{\bullet-} \longrightarrow {}^-OS(O)_2OCH_2{-}\dot{C}HR;$$

and hydrogen atom abstraction,

$$RH + SO_4^{\bullet-} \longrightarrow R^{\bullet} + HSO_4^-$$

The absolute reactivity of SRA in the last reaction was studied using the flash photolysis technique and was characterized by the SRA consumption rate in the presence of various concentrations of an organic compound. Nearly all of the known rate constants of hydrogen atom abstraction from organic molecules by SRA are presented in [6–18] and in our works [19–21]. The data array available on the reactivity of SRA provides insight into the H atom abstraction reactions.

Here, we analyze kinetic data in terms of the intersecting parabolas model (IPM), which was suggested by Denisov [22–24]. This model was successfully used in kinetic studies of homolytic hydrogen atom abstraction from a wide variety of organic molecules by free radicals [25, 26]. The IPM method enables one to quantitatively estimate the kinetic effects of various factors (solvent, multidipole interaction, etc.) by comparing the IPM parameters of the reaction examined to the same parameters of a reference reaction in which this effect is not observed.

The interaction between SRA and an organic molecule takes place in aqueous media. It is, therefore, expected a priori that the solvent will exert a strong effect on the reaction rate. However, there are no kinetic data for the reference (gas-phase) reaction. For this reason, the IPM parameters for the gas-phase reaction are calculated here using density functional theory. This approach was validated in recent works [27–30], including for SRA [31].

METHODS

Denisov's intersecting parabolas model considers hydrogen atom abstraction by a free radical,

$$RH + X^{\bullet} \longrightarrow R^{\bullet} + XH,$$

as a result of the intersection of two energy curves, namely, the parabola describing the potential energy of the stretching vibrations of the breaking bond in RH and the parabola describing the potential energy of the stretching vibrations of the forming bond in the reaction product XH [22–25]. The key IPM equation is

$$br_e = \alpha(E_e - \Delta H_e)^{1/2} + E_e^{1/2}, \quad (1)$$

where $2b^2$ is the force constant of the C–H bond being attacked, $b = \pi\nu(2\mu)^{1/2}$, μ is the reduced mass of the atoms forming the bond, and r_e is the H atom transfer distance in the elementary event. Since b depends only slightly on the surroundings of the C–H bond being attacked, the quantity br_e can be used to characterize various abstraction reactions involving free radicals, including the reactions examined here. The value of r_e depends on the strength of the breaking bond or, in other terms, on the heat of the reaction (ΔH_e):

$$\Delta H_e = \Delta D + \Delta ZPE, \quad (2)$$

where ΔD is the difference between the dissociation energies of the breaking and forming bonds and ΔZPE is the difference between the zero point energies of these bonds. In Eq. (1), α is the square root of the ratio of the force constants of the breaking and forming bonds and E_e is the activation energy related to the experimentally determinable activation energy E_a by the equation

$$E_e = E_a + ZPE - RT/2. \quad (3)$$

Thus, the following data are necessary for an IPM analysis of the experimental rate constant data array: D(C–H) data for the substrates, $D(H–OSO_3^-)$, the stretching frequencies ν(C–H) and ν(O–H), and the activation energies of the reactions to be examined.

The values of D(C–H) were either taken from [32] or calculated from the enthalpies of formation of $R^{\bullet}$ and RH [32, 33]. For compounds for which these data were lacking, we assumed that the dissociation energy of the secondary C–H bond remote from the polar group is 394.2 kJ/mol, as in $CH_3C\underline{H}_2CH_2OH$. The dissociation energy of the α-CH_2 bond in ethers was taken to be equal to the dissociation energy of the same bond in diethyl ether (385.0 kJ/mol). The dissociation energy of the tertiary C–H bond in the α-position with respect to the oxygen atom in ethers and alcohols was taken to be equal to D(C–H) for isopropanol (379.1 kJ/mol).

According to [34], the standard enthalpy of formation of SRA is $\Delta_f H^\circ(SO_4^{\bullet-}) = -737.6 \pm 9.6$ kJ/mol. Two enthalpy values are known for the hydrosulfate anion: $\Delta_f H^\circ = -981 \pm 13$ [35] and -967 ± 11 kJ/mol [36]. Hence, $D(H–OSO_3^-) = 461 \pm 16$ or 447 ± 15 kJ/mol. The calculation of the $H–OSO_3^-$ bond dissociation energy by the G2, G3, and G2MP2 composite methods yields 445.8, 440.6, and 448.0 kJ/mol, respectively, corroborating the value reported in [36]. For this reason, we used $D(H–OSO_3^-) = 445.8$ kJ/mol in further calculations.

The stretching frequencies of C–H bonds were calculated in the B3LYP/6-31G(d, p) approximation. The ν(O–H) value for the hydrosulfate anion was found by the B3LYP/6-311+G(d, p) method. The well-known systematic positive error in the calculated vibration frequencies was corrected by multiplying them by a coefficient of 0.9806 [37]. When there were composite vibrations, which are mainly typical of secondary and primary C–H bonds, the lowest frequency of symmetric C–H vibrations was used in the IPM scheme. We found that ν(O–H) = 3738 cm^{-1}. The ν(C–H) value depends only slightly on the nearest neighbors of the C–H bond and lies within the rather narrow range of 2900–3100 cm^{-1}.

Activation energies were either taken from experimental data or calculated using the equation

$$E_a = RT\ln(A_p/k_p). \quad (4)$$

An analysis of preexponential factor data for $SO_4^{\bullet-}$ + RH $\longrightarrow$ HSO_4^- + $R^{\bullet}$ reactions involving various organic compounds [6–18, 20] indicates that the partial quantity A_p is independent of the degree of substitution of the carbon atom of the C–H bond and of the nearest neighbors of the bond attacked. The average value of this quantity derived from 15 measurements, $\log A_p = 9.77 \pm 0.36$, was used in Eq. (4) to calculate activation energies from partial rate constants.

Some of the most typical values of the partial rate constant k_p for the reactions of SRA with different types of C–H bonds are listed in Table 1. For compounds with nonequivalent C–H bonds, we calculated k_p for the bond indicated in Table 2, using the overall rate constant of the reaction $SO_4^{\bullet-}$ + RH [6–21] and known partial rate constants (Table 1).

Quantum chemical calculations were done using the Gaussian 98 program (version A.7) [38]. The unrestricted Kohn–Sham method in the B3LYP/6-311+G(d, p) approximation was used in free radical calculations and in the transition state (TS) location. We demonstrated in an earlier publication [31] that this level of complexity is sufficient for high-accuracy calculation of the activation energy of hydrogen atom abstraction from various types of C–H bonds by free radicals: with a few exceptions, which are noted in [31], the mean absolute error of E_a calculation is as small as 3.3 kJ/mol and the maximum deviation is no larger than 10 kJ/mol. Transition states were sought using the QST2 and QST3 algorithms [39]. Each TS was verified by obtaining one negative frequency as a solution of the vibrational problem.

Table 1. Partial rate constants (k_p) of hydrogen atom abstraction from various C–H bonds by the sulfate radical anion (T = 295 K)

Bond attacked	Initial compound	k_p, l mol^{-1} s^{-1}
C<u>H</u>$_3$–	CH_3CH_3	7.3×10^5
C<u>H</u>$_3$–O–	CH_3OH	3.3×10^6
C<u>H</u>$_3$–C–O–	$(CH_3)_3COH$	9.3×10^4
C<u>H</u>$_3$–C(O)–	$CH_3C(O)CH_3$	1.6×10^4
C<u>H</u>$_3$–NO_2	CH_3NO_2	8.7×10^3
C<u>H</u>$_3$–C(O)O–	$CH_3C(O)OH$	4.7×10^3
C<u>H</u>$_3$–CN	CH_3CN	1.6×10^3
C<u>H</u>$_3$–S(O)$_2$–	$CH_3S(O)_2CH_3$	5.7×10^2
–C<u>H</u>$_2$–	$CH_3CH_2CH_3$	1.8×10^7
–C<u>H</u>$_2$–O–	CH_3CH_2OH	2.1×10^7
–C<u>H</u>$_2$–CH_2–O–	$CH_3CH_2CH_2OH$	7.0×10^6
–C<u>H</u>$_2$–OC(O)–	$CH_3CH_2OC(O)CH_3$	1.2×10^6
–C<u>H</u>$_2$–C(O)–	$CH_3CH_2C(O)CH_3$	7.8×10^5
–C<u>H</u>$_2$–Cl	$ClCH_2CH_2Cl$	4.0×10^5
>C<u>H</u>–	$(CH_3)_3CH$	1.0×10^8
>C<u>H</u>–O–	$(CH_3)_2CHOH$	8.1×10^7
>C<u>H</u>–CH_2–O–	$(CH_3)_2CHCH_2OH$	8.3×10^7

By scanning the potential energy surface along the intrinsic reaction coordinate (standard IRC procedure), it was demonstrated for all cases that the imaginary frequency corresponds to the transfer of a hydrogen atom from the oxidation substrate to SRA. We examined the transition states of the reactions of SRA with aliphatic hydrocarbons, chloromethanes, methanol, acetone, acetonitrile, nitromethane, and dimethylsulfone.

The activation energies of hydrogen atom transfer reactions were calculated as the difference between the standard enthalpy of the TS and the sum of the standard enthalpies of SRA and the compound attacked. The total energy of a compound was converted to H°_{298} by adding, to E_{total}, the zero point energy (*ZPE*), the work of the expansion of 1 mol of the ideal gas (*RT*), and the thermal correction energy ($H^\circ_{298} - H^\circ_0$) calculated using equations of statistical thermodynamics. The solvent effect on the activation energy was taken into account using the continuum model CPCM (COSMO) [40].

RESULTS AND DISCUSSION

The kinetic data listed in Tables 1 and 2 indicate that the reactivity of the C–H bond depends considerably on the oxidation substrate (RH) structure. Note the following interesting points:

(1) In earlier works [17, 19, 20], it was found for small sets of similar compounds that $\log k_p$ increases linearly with an increasing strength of the bond attacked. However, it follows from the data presented in Table 1 that the reactivity of the unactivated C–H bond is approximately equal to the reactivity of the C–H bonds having an oxy group in the α-position with respect to the reaction center (as in alcohols and ethers), although these types of bonds differ markedly in strength. These observations can be explained by the dual effect of the neighbor O atom on the reactivity of the C–H bond: on the one hand, the O atom increases k_p by reducing the D(C–H) value; on the other hand, owing to its polar properties, the oxygen-containing substituent exerts the opposite effect, reducing the partial rate constant. The origin of the deactivating effect of polar groups will be discussed below.

(2) The reactivity of the β-C–H bonds of alcohols and ethers is somewhat lower than the reactivity of unactivated C–H bonds and α-C–H bonds. The difference is the largest for primary C–H bonds and is nearly zero in compounds with tertiary C–H bonds (Table 1). Since the β-C–H bonds of alcohols and ethers and the C–H bonds of hydrocarbons have similar strengths and since saturated systems show low conductivity with respect to the inductive effect of the polar group, the decrease of k_p can be attributed to the solvation (hydration) of the alcohol or ether molecule, an effect unfavorable for the reaction.

(3) The introduction of a highly polar substituent (–C(O)–, –C(O)O–, –NO_2, –S(O)$_2$–, or –CN) into the oxidation substrate RH reduces k_p, and this effect cannot be attributed to the change in D(C–H) alone.

Thus, k_p depends both on D(C–H) and on the polarity of the substituent X. The effect of the latter is manifested either directly, through the interaction between SRA with the electric field of the molecule (ion–dipole interaction), or indirectly, as the X-dependent difference between the hydration energies of the oxidation substrate and the TS. It is difficult to separate and quantitatively evaluate these latter effects in the framework of conventional correlations, and this is the reason why we used Denisov's method.

Kinetic analysis of the reaction $SO_4^{\bullet-}$ + RH by the intersecting parabolas method. Regarding the kinetic data as a whole, note that the partial rate constant varies in a wide range of over 5 orders of magnitude. Wide variation ranges are also observed for the activation energy (up to 30 kJ/mol) and for the C–H bond strength in the compounds examined. Table 2 lists calculated data for organic compounds of different classes, including hydrocarbons and molecules containing various polar groups; that is, the kinetic data array is rather heterogeneous. The large difference between the nature of the C–H bond attacked and the nature of its nearest

Table 2. Kinetic characteristics of the $SO_4^{\bullet -}$ + RH reactions and the key IPM parameters*

RH	$\log A_p$ E_a or ($\log k_p$)	ΔH_e	α	br_e	$E_{e,0}$	ΔE_Σ
Primary C–H bond						
CH_3CH_3	(5.87)	–37.0	0.786	13.05	53.4	–22.2
CH_3OH	10.15 18.2	–48.9	0.776	12.97	53.3	–23.1
CH_3OD	(6.56)	–48.9	0.776	12.96	53.2	–23.2
$(CH_3)_3COH$	(4.97)	–30.3	0.787	13.39	56.1	–19.4
$(CH_3)_3COCH_3$	(6.91)	–60.1	0.779	13.21	55.2	–21.0
$CH_3C(O)CH_3$	6.90 15.0	–57.0	0.790	13.06	53.2	–22.1
CH_3CN	6.10 16.0	–60.6	0.795	13.41	55.8	–19.0
CH_3NO_2	8.10 22.0	–34.6	0.803	13.12	53.0	–21.2
$HOC(CH_3)_2C(CH_3)_2OH$	(5.34)	–37.1	0.780	13.36	56.3	–19.8
$CH_3C(O)OC(CH_3)_3$	(5.22)	–35.2	0.793	13.50	56.7	–18.3
$CH_3S(O)_2CH_3$	(2.75)	–9.2	0.798	13.99	60.5	–14.1
$CH_3C(O)OH$	(3.67)	–42.6	0.797	14.89	68.6	–6.1
Unactivated secondary C–H bond						
$CH_3CH_2CH_3$	(7.25)	–50.9	0.783	12.62	50.1	–19.7
$CH_3CH_2CH_2OH$	(6.85)	–56.0	0.792	13.25	54.7	–14.5
$CH_3CH_2CH_2CH_2OH$	(7.04)	–56.2	0.785	13.03	53.3	–16.4
$CH_3CH_2(CH_2)_3OH$	(7.39)	–56.2	0.786	12.78	51.2	–18.4
cyclo-((CH_2)$_2$CH(OH)(CH_2)$_2$–)	(7.39)	–55.9	0.796	12.89	51.5	–17.3
$CH_3CH_2(CH_2)_4OH$	(7.18)	–56.2	0.786	12.94	52.5	–17.1
cyclo-((CH_2)$_3$CH(OH)(CH_2)$_2$–)	9.86 8.3	–56.2	0.785	12.05	45.6	–24.1
$CH_3CH_2(CH_2)_5OH$	(7.65)	–56.2	0.786	12.58	49.6	–19.9
$CH_3CH_2(CH_2)_6OH$	(7.54)	–56.2	0.786	12.66	50.3	–19.3
$(CH_3CH_2CH_2)_2O$	(7.45)	–56.4	0.774	12.59	50.4	–20.1
cyclo-(–(CH_2)$_5$O–)	10.01 11.1	–56.1	0.789	12.49	48.7	–20.6
cyclo-(–(CH_2)$_6$O–)	9.65 7.3	–55.9	0.796	12.02	44.8	–24.0
cyclo-(–CH_2(CH_2)$_2$C(O)(CH_2)$_2$–)	9.73 11.3	–56.1	0.789	12.51	48.9	–20.4
cyclo-(–$CH_2CH_2C(O)CH_2CH_2$–)	9.52 11.6	–56.0	0.793	12.59	49.4	–19.7
$CH_3COOCH_2(CH_2)_3CH_3$	(6.94)	–56.2	0.786	13.12	53.9	–15.6
$AcOCH_2CH_2CH_2OAc$	(6.16)	–56.0	0.794	13.76	58.8	–10.1
$AcOCH_2CH_2CH_2CH_2OAc$	(6.46)	–56.0	0.791	13.52	56.9	–12.2
$AcO(CH_2)_2CH_2(CH_2)_2OAc$	(7.18)	–56.1	0.788	12.96	52.6	–16.8
Activated secondary C–H bond						
CH_3CH_2OH	10.18 14.6	–63.6	0.773	13.06	54.2	–16.3
$(CH_3)_3CCH_2OH$	(6.96)	–63.7	0.771	13.21	55.6	–15.1
$(CH_3CH_2)_2O$	(7.05)	–65.8	0.767	13.19	55.7	–15.3
cyclo-(–(CH_2)$_3$O–)	10.31 13.2	–65.1	0.796	13.23	54.3	–14.5
cyclo-(–(CH_2)$_4$O–)	(7.12)	–64.9	0.808	13.62	56.7	–11.1
$ClCH_2CH_2OH$	(6.71)	–63.5	0.781	13.51	57.6	–12.4
$HOCH_2OH$	9.03 10.8	–69.2	0.786	12.95	52.6	–17.0
(–CH_2CH_2O–)$_n$–	(6.88)	–65.8	0.767	13.31	56.7	–14.3
cyclo-(–(CH_2)$_2$O(CH_2)$_2$O–)	(6.63)	–65.6	0.777	13.60	58.6	–11.7
cyclo-(–(CH_2)$_2$O(CH_2)$_2$O–)	9.84 12.7	–65.6	0.777	12.93	53.0	–17.3
CH_2Cl_2	(5.72)	–37.6	0.814	13.51	55.4	–12.0

Table 2. (Contd.)

RH	$\log A_p$ E_a or ($\log k_p$)	ΔH_e	α	br_e	$E_{e,0}$	ΔE_Σ
$C\underline{H}_2ClC\underline{H}_2Cl$	9.95 21.0	–37.8	0.809	13.21	53.3	–14.5
$CH_3C(O)OC\underline{H}_2CH_3$	(6.08)	–57.8	0.797	13.93	60.1	–8.7
$AcO(C\underline{H}_2)_2OAc$	(5.54)	–57.8	0.798	14.30	63.3	–5.4
$CH_3C(O)C\underline{H}_2CH_3$	(5.89)	–69.5	0.793	14.46	65.1	–4.0
Unactivated tertiary C–H bond						
$(CH_3)_3C\underline{H}$	(8.01)	–58.1	0.777	12.27	47.7	–14.1
$(CH_3)_2C\underline{H}CH_2OH$	(7.92)	–65.4	0.787	12.78	51.1	–10.0
$CH_3COOCH_2C\underline{H}(CH_3)_2$	(7.38)	–65.4	0.787	13.18	54.4	–6.7
Activated tertiary C–H bond						
$(CH_3)_2C\underline{H}OH$	9.18 7.2	–71.6	0.770	12.35	48.6	–13.6
$(C_2H_5)_2C\underline{H}OH$	(8.11)	–71.7	0.766	12.62	51.0	–11.5
$((CH_3)_2C\underline{H})_2O$	(8.00)	–71.5	0.779	12.85	52.2	–9.5
$C\underline{H}Cl_3$	(6.61)	–44.8	0.829	13.38	53.5	–4.8

* The experimental activation energy (E_a), the heat of the reaction (ΔH_e), the activation energy of the thermally neutral reaction ($E_{e,0}$), and the overall energy of the polar interaction (ΔE_Σ) are in kJ/mol. The partial rate constants at 295 K and the preexponential factors are in l mol^{-1} s^{-1}. The parameter br_e has dimensions of (kJ/mol)$^{1/2}$.

neighbors dictates that this array should be divided into more homogeneous groups. It is most natural to divide the data array into groups according to the kind of C–H bond for which the partial rate constant of hydrogen atom abstraction is calculated, so we will distinguish primary C–H bonds (group 1), secondary C–H bonds (group 2), and tertiary C–H bonds (group 3).

Group 1. This group of compounds as a whole is characterized by the highest strength of the breaking bond and the widest range of partial rate constant values (from 5.7×10^2 l mol^{-1} s^{-1} for $C\underline{H}_3S(O)_2C\underline{H}_3$ to 8.1×10^6 l mol^{-1} s^{-1} for $((CH_3)_3COC\underline{H}_3)$). Nevertheless, the parameter br_e varies only slightly with the nature of RH. The presence of a highly polar substituent (–CN, –OC(O)R', or $–S(O)_2–$) in the molecule causes an increase in br_e. For the other compounds, br_e is nearly constant and is 13.14 ± 0.17 (kJ/mol)$^{1/2}$.

Group 2. This group includes hydrocarbons, alcohols, ethers, esters, cyclic oxygen-containing compounds, and other compounds with various distances between the secondary C–H bond attacked and the polar group. A primary analysis of kinetic data has demonstrated that the parameter br_e varies rather widely in this group. A more detailed analysis shows that the proximity of the polar group to the reaction center has an effect on the key IPM parameters. For this reason, the second group was further divided into a subgroup of compounds in which the secondary C–H bond attacked is remote from the polar moiety (unactivated) and a subgroup of compounds in which this bond is activated. After this subdivision, it turns out that br_e is nearly invariable within either subgroup. Again, the exception is the compounds with a highly polar compound. In this case, these are monoatomic and diatomic esters and methyl ethyl ketone. For the other compounds, it was found that $br_e = 12.64 \pm 0.34$ (kJ/mol)$^{1/2}$ for unactivated C–H bonds and $br_e = 13.28 \pm 0.24$ (kJ/mol)$^{1/2}$ for α-C–H bonds.

Group 3. An essentially similar situation is observed in this group: the tertiary α-C–H bonds are simultaneously activated (D(C–H) is decreased) and deactivated (k_p is changed only slightly), and polar substituents increase the br_e value. However these regularities were established on the basis of a limited number of examples.

It is clear from the above analysis that br_e depends on a number of factors other than the strength of the breaking C–H bond. The following factors can be deduced from general considerations: the effect of the solvent as a polarized isotropic medium and as a specific solvating agent capable of forming hydrogen bonds with SRA, with the polar molecule, and with the TS; the electrostatic interaction between the $SO_4^{\bullet-}$ anion with polar groups (ion–dipole interaction), which includes the multidipole interaction for some substrates (e.g., diatomic esters). In the framework of IPM, the

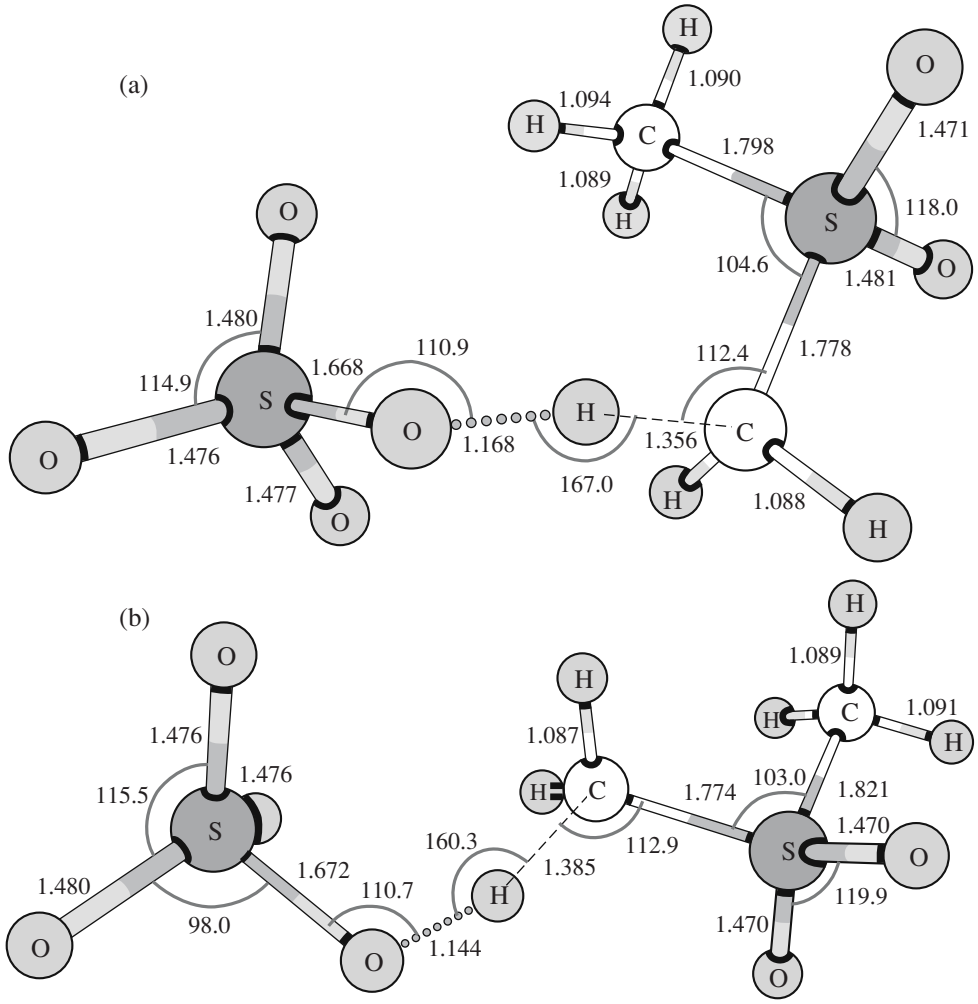

Fig. 1. Transition state of the reaction between the sulfate radical anion and dimethylsulfone: reactant orientations (a) favorable and (b) unfavorable for ion–dipole interaction energy minimization (see text). The calculation was carried out in the B3LYP/6-311+G(*d*, *p*) approximation. The single imaginary vibration frequency is (a) 1716i and (b) 1596i cm^{-1}.

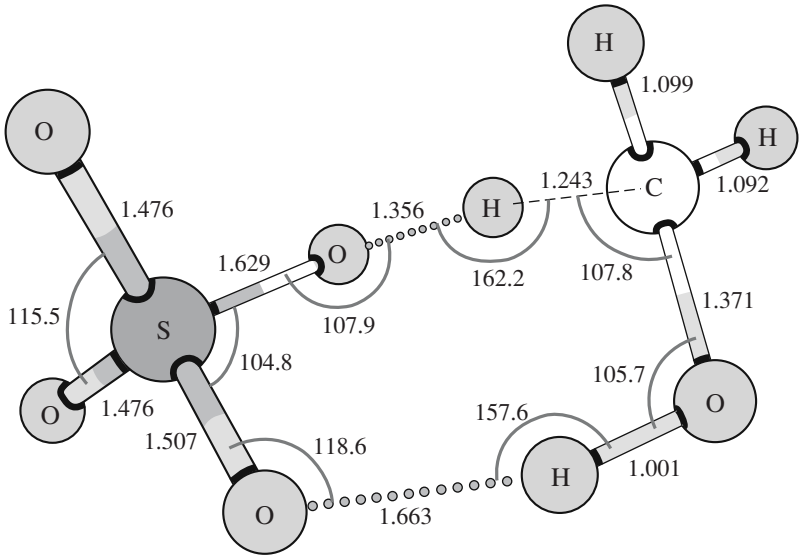

Fig. 2. Formation of an intramolecular hydrogen bond in the transition state of the reaction between the sulfate radical anion and methanol. The calculation was carried out in the B3LYP/6-311+G(*d*, *p*) approximation. The single imaginary vibration frequency is 1119i cm^{-1}.

Table 3. Calculated gas-phase br_e data and the changes of solvation energy for the reaction $SO_4^{\bullet-}$ + RH

RH	$(br_e)_{RH,\,g}$, $(kJ/mol)^{1/2}$	ΔE_{solv}(IPM)*	Contributions to ΔE_{solv}(COSMO), kJ/mol		
			electrostatic	nonelectrostatic	overall
C_2H_6	15.53	–22.2	–18.3	2.4	–15.9
$CH_3C\underline{H}_2CH_3$	14.90	–19.7	–20.2	4.7	–15.5
$(CH_3)_3C\underline{H}$	13.97	–14.1	–15.9	5.8	–10.1
CH_2Cl_2	12.54	7.7	12.3	7.7	20.0
$CHCl_3$	12.35	7.9	20.4	10.9	31.3
$(CH_3)_2CO$	12.42	5.1	22.9	6.7	29.6
CH_3CN	12.65	6.1	31.3	3.3	34.7
CH_3NO_2	11.85	9.8	38.5	6.3	44.8
$(CH_3)_2SO_2$	8.97	35.6	47.9	5.1	53.0

* Calculated using Eq. (5) and $(br_e)_{RH,l}$ and α data from Table 2.

energy of any effect changing the kinetics of the reaction is calculated as

$$\Delta E = \frac{(br_e)^2_{effect} - (br_e)^2_{no\_effect}}{(1+\alpha)^2}; \qquad (5)$$

that is, this calculation requires kinetic data for systems in which the effect examined is not observed.

In order to take into account the solvent effect, it is necessary to have kinetic data for the gas-phase reaction $SO_4^{\bullet-}$ + RH. Because of the lack of these data, we used the results of quantum chemical simulations in the B3LYP/6-311+G(*d*, *p*) approximation for the transition states of the reactions of SRA with ethane, propane, isobutane, dichloromethane, trichloromethane, methanol, acetone, acetonitrile, nitromethane, and dimethylsulfone. The TS structure for the reactions of SRA with dimethylsulfone and methanol are shown in Figs. 1 and 2, respectively.

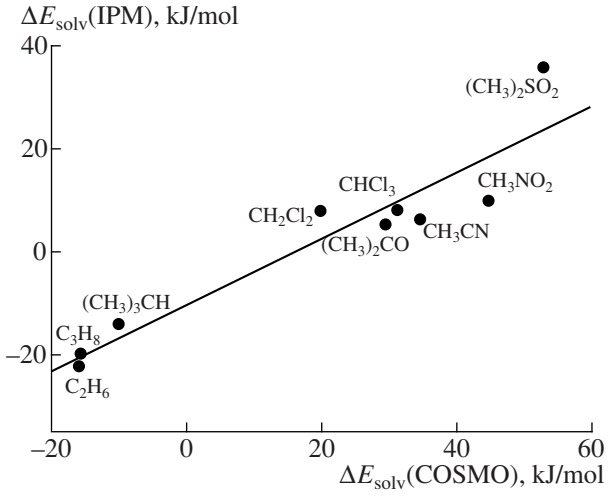

Fig. 3. Comparison of the energy effects in two solvation models for the reactions of the sulfate radical anion with organic compounds.

The effect of the nature of the organic compound on the structure of the $SO_4^{\bullet-}$ + RH reaction center was discussed in detail in our earlier work [31]. For this reason, we will focus only on the reactivity of different C–H bonds. In the calculation of the activation energies of the reactions examined, we took into account the zero point energies of the transition states and reactants and converted the results to 298 K. This approach enabled us to calculate the parameter br_e for gas-phase reactions using Eq. (1) and to calculate the energy of solvation of the reaction center (ΔE_{solv}(IPM)) using Eq. (5). The results of these calculations are presented in Table 3. The br_evalues for the aqueous phase were taken from Table 2. The calculation of ΔE_{solv}(IPM) demonstrates that passing from the gas phase to the aqueous phase facilitates the interaction of SRA with nonpolar compounds, primarily hydrocarbons; that is, SRA exerts a kind of solubilizing effect on the TS of the reaction.

Here the following question arises: Which component of ΔE_{solv} (specific or nonspecific) is dominant? In aqueous solution, which is a strongly associated medium, the formation of hydrogen bonds with the reactants and the TS obviously takes place. However, the problem of simulating these processes is much complicated. For this reason, we used a simpler approach consisting in estimating the contribution from nonspecific solvation to ΔE_{solv}. The effect of the nonspecific solvation of the reaction center was studied in the framework of the polarized continuum model CPCM (COSMO) [40]. The calculated ΔE_{solv}(COSMO) data are listed in Table 3.

The ΔE_{solv} values calculated using the independent methods IPM and COSMO are satisfactorily correlated (Fig. 3), suggesting that the major role is played by

Table 4. Calculated ion–dipole interaction energies

RH	$\Delta E_\Sigma - \Delta E_{solv}$, kJ/mol	Point-charge model			
		θ, deg	r, Å	μ≠, D	E_{i-d}, kJ/mol
C_2H_6	0.0	26.6	3.75	1.66	30.5
$CH_3C\underline{H}_2CH_3$	0.0	13.1	4.01	1.19	20.9
$(CH_3)_3C\underline{H}$	0.0	19.9	3.84	0.83	15.3
CH_2Cl_2	–19.7	175.1	3.12	0.76	–22.4
$CHCl_3$	–12.7	149.8	3.30	1.18	–27.0
$(CH_3)_2CO$	–27.1	126.6	3.89	5.24	–59.7
CH_3CN	–25.2	151.8	3.84	3.47	–59.9
CH_3NO_2	–31.0	156.3	4.09	5.86	–92.7
$(CH_3)_2SO_2$	–49.7	165.1	4.12	7.58	–125.0

nonspecific solvation due to the electrostatic component (Table 3). However, specific solvation cannot be neglected for compounds. For example, the data calculated for methanol fall out of the correlation. Unlike the other reactants, methanol forms a hydrogen bond with the radical anion in the TS (Fig. 2). It is likely that specific solvation will also play a great reactivity-regulating role for the other alcohols in which the α-C–H bond is attacked.

The values of $(br_e)_{RH,l}$ derived from kinetic data indicate that this parameter is affected by at least two factors, namely, solvation by water molecules and the polar interaction between SRA and the functional groups of RH. Neither effect is involved in the calculation of $(br_e)_{HC,g}$, the IPM parameter for the hydrocarbon in the gas phase. Therefore, the energy effect ΔE_Σ calculated using the equation

$$\Delta E_\Sigma = \frac{(br_e)^2_{RH,1} - (br_e)^2_{HC,g}}{(1+\alpha)^2} = \frac{(br_e)^2_{RH,1} - (br_e)^2_{RH,g}}{(1+\alpha)^2} + \frac{(br_e)^2_{RH,g} - (br_e)^2_{HC,g}}{(1+\alpha)^2} = \Delta E_{solv} + \Delta E_{i-d}$$

is equal to the sum of the solvation energy and the ion–dipole interaction energy. Using the earlier determined ΔE_{solv}(IPM) value (Table 3) and the ΔE_Σ value presented in Table 2, it is possible to calculate the ion–dipole interaction energy ΔE_{i-d} for the TS of the reaction $SO_4^{\bullet-}$ + RH (Table 4).

In order to verify these results, we estimated the ion–dipole interaction energy by an independent method. Provided that the ion–dipole distance is much longer than the dipole length (the distance between the negative and positive charge centers), the ion–dipole interaction energy is

$$E_{i-d} = -\frac{1}{4\pi\varepsilon\varepsilon_0}\frac{q\mu\cos\theta}{r^2}, \quad (6)$$

where ε_0 is the electric constant, ε is the dielectric constant of the medium (taken to be equal to unity in our calculations), q is the charge of the ion, μ is the dipole moment, r is the distance between the ion and the dipole center, and θ is the angle between the dipole axis and the straight line r. Using the calculated geometric parameters of transition states, we determined r and cosθ for the compounds examined (Table 4). The ion–dipole interaction energy was calculated under the simplest assumption that the dipole moment of the RH

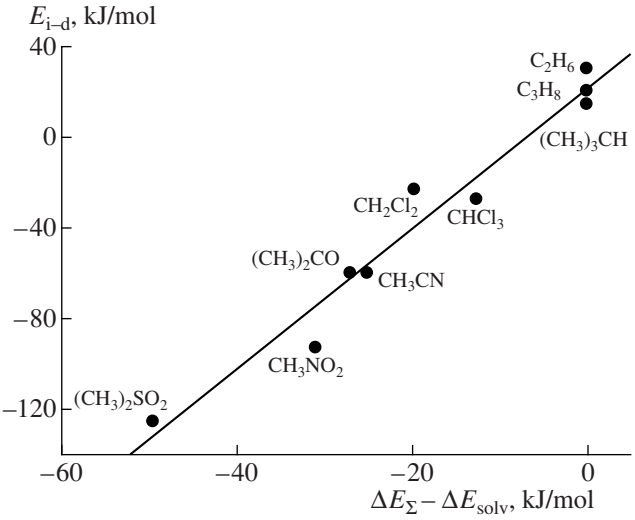

Fig. 4. Correlation between the independent estimates of the ion–dipole interaction energy in the transition state of hydrogen atom abstraction from various organic molecules by the sulfate radical anion.

molecule can be calculated in the point-charge approximation. Atomic charges were determined by the natural bond orbital (NBO) analysis of electron distribution [41] since the Mulliken analysis of electron densities often yields incorrect results, particularly for augmented basis sets that include diffuse functions [42]. Another reason why the dipole moment was calculated in the point-charge approximation is that, in the transition state, the RH molecule is polarized in the field of the radical anion. As a consequence the dipole moment of the molecule in the transition state is very different from that of the isolated molecule.

The calculated E_{i-d} data are presented in Table 4. There is a correlation between the two independent estimates of the ion–dipole interaction energy (Fig. 4). Taking into account the above assumptions, this correlation should be viewed as quite satisfactory. For the above-mentioned reasons, the data for methanol are excluded from the correlation. The E_{i-d} values obtained from Eq. (7) are overestimated because of the neglect of ε and the error arising from the computational approximations. The observed correlation points to the great role of the ion–dipole interaction in the regulation of the reactivity of C–H bonds in their reactions with $SO_4^{\bullet-}$. This role is particularly clear from the comparison between the two transition states of the reaction between SRA and dimethylsulfone (Fig. 1). The difference between the mutual orientations of the radical anion and the dimethylsulfone dipole causes a significant difference between the corresponding gas-phase activation energies: for TS1, $\theta = 165.1°$ and E_a = 4.2 kJ/mol; for the less favorable orientation in TS2 ($\theta = 122.2°$), the activation energy has a much larger value of 36.6 kJ/mol.

In the light of these concepts, it is clear why the br_e value for esters is larger than the average br_e value for their respective groups (Table 2). The mutual orientation of the ester group dipoles and the radical anion is unfavorable for the reaction. This reduce the observed rate constant, thus increasing the br_e value. As the distance between the ester groups in the series of $AcO(CH_2)_nOAc$ compounds (n = 2–5) increases, br_e decreases systematically because of the weakening effect of the ion–dipole interaction.

Thus, using Denisov's intersecting parabolas method, we have analyzed a large array of experimental rate constant data for the reactions of the sulfate radical anion $SO_4^{\bullet-}$ with the C–H bonds of hydrocarbons; alcohols; ketones; ethers; esters; and chlorine-, nitrogen-, and sulfur-containing organic compounds in water. It was found by comparing key IPM parameters that br_e depends systematically on the degree of substitution of the C–H bond attacked. Within certain groups of compounds, br_e is constant and it is, therefore, possible to use this parameter as a measure of the reactivity of C–H bond types. A polar group adjacent to the secondary or tertiary C–H bond being attacked increases br_e. This effect is not observed for primary C–H bonds. The transition states of the reaction have been located in the B3LYP/6-311+G(d, p) approximation for ten organic compounds, and the activation energies of the reaction $SO_4^{\bullet-}$ + RH have been calculated. Using these data, the IPM parameters for the gas phase have been determined and the energy changes upon the hydration of the transition state and reactants have been estimated. Passing from the gas phase to an aqueous medium facilitates the interaction of SRA with nonpolar compounds, particularly hydrocarbons. The solvation energy calculation by the polarized continuum method has demonstrated that a significant contribution to the overall solvent effect is made by the nonspecific solvation of the reactants. The ion–dipole interaction energy in the transition state has been calculated by independent methods (IPM and the point-charge model), and it has been demonstrated that this energy is the determining factor in the TS structure and energy for the reactions of $SO_4^{\bullet-}$ with polar organic compounds.

ACKNOWLEDGMENTS

This work was supported by the Ministry of Education and Science of the Russian Federation through the departmental analytical purpose program "Development of the Scientific Potential of Higher Schools (2006–2008)," project RNTs 2.2.1.1.6332.

REFERENCES

1. Eliseeva, V.I., Ivanchev, S.S., Kuchanov, S.I., and Lebedev, A.V., *Emul'sionnaya polimerizatsiya i ee primenenie v promyshlennosti* (Emulsion Polymerization and Its Commercial Applications), Moscow: Khimiya, 1976.
2. Walling, Ch., *Free Radicals in Solution*, New York: Wiley, 1956.
3. Heidt, L.J., *J. Chem. Phys.*, 1942, vol. 10, no. 2, p. 297.
4. Hart, E.J., *J. Am. Chem. Soc.*, 1961, vol. 83, no. 3, p. 567.
5. Pikaev, A.K., Shilov, V.P., and Spitsyn, V.I., *Radioliz vodnykh rastvorov lantanidov i aktinidov* (Radiolysis of Aqueous Solutions of Lanthanides and Actinides), Moscow: Nauka, 1983.
6. Ball, D.L., Crutchfield, M.M., and Edwards, J.O., *J. Org. Chem.*, 1960, vol. 25, no. 9, p. 1599.
7. Ball, D.L., *Chem. Abstr.*, 1957, vol. 51, nos. 13–15, p. 9272.
8. Bartlett, P.D. and Cotman, J.D., *J. Am. Chem. Soc.*, 1949, vol. 71, no. 4, p. 1419.
9. Kolthoff, I.M., Meehan, E.J., and Carr, E.M., *J. Am. Chem. Soc.*, 1953, vol. 75, no. 6, p. 1439.
10. Levitt, L.S. and Malinowski, E.R., *J. Am. Chem. Soc.*, 1955, vol. 77, no. 17, p. 4517.
11. Levitt, L.S. and Malinowski, E.R., *J. Am. Chem. Soc.*, 1956, vol. 78, no. 9, p. 2018.
12. Malinowski, E.R. and Levitt, L.S., *J. Am. Chem. Soc.*, 1958, vol. 80, no. 20, p. 5334.
13. Wiberg, K.B., *J. Am. Chem. Soc.*, 1959, vol. 81, no. 1, p. 252.

14. Ozawa, T. and Kwan, T., *Polyhedron*, 1983, vol. 2, no. 10, p. 1019.
15. Eibenberger, H., Steenken, S., O'Neill, P., and Schultze-Frohlinde, D., *J. Phys. Chem.*, 1978, vol. 82, no. 6, p. 749.
16. Clifton, C.L. and Huie, R.E., *Int. J. Chem. Kinet.*, 1989, vol. 21, p. 677.
17. Huie, R.E. and Clifton, C.L., *Int. J. Chem. Kinet.*, 1989, vol. 21, p. 611.
18. Davies, M.J., Gilbert, B.C., Thomas, C.B., and Young, J., *J. Chem. Soc., Perkin Trans. 2*, 1985, no. 8, p. 1199.
19. Khursan, S.L. and Nikolaev, A.I., *Khim. Fiz.*, 1990, vol. 10, no. 3, p. 317.
20. Zapol'skikh, V.V., Safiullin, R.L., Khursan, S.L., Teregulova, A.N., Zaripov, R.N, and Komissarov, V.D., *Khim. Fiz.*, 2001, vol. 20, no. 3, p. 58.
21. Zapol'skikh, V.V., Safiullin, R.L., Khursan, S.L., and Teregulova, A.N., *Bashkir. Khim. Zh.*, 1998, vol. 5, no. 4, p. 24.
22. Denisov, E.T., *Usp. Khim.*, 1997, vol. 66, no. 10, p. 953.
23. Denisov, E.T., *Kinet. Katal.*, 1991, vol. 32, no. 2, p. 461.
24. Denisov, E.T., in *General Aspects of the Chemistry of Radicals*, Alfassi, Z.B., Ed., New York: Wiley, 1999, p. 79.
25. Denisov, E.T. and Denisova, T.G., *Handbook of Antioxidants*, Boca Raton, Fla.: CRC, 2000, p. 289.
26. Denisov, E.T., Denisova, T.G., and Pokidova, T.S., *Handbook of Free Radical Initiators*, Hoboken: Wiley, 2003, p. 879.
27. Shestakov, A.F., Denisova, T.G., Denisov, E.T., and Emel'yanova, N.S., *Izv. Akad. Nauk, Ser. Khim.*, 2002, no. 4, p. 559.
28. Shestakov, A.F. and Denisov, E.T., *Izv. Akad. Nauk, Ser. Khim.*, 2003, no. 2, p. 306.
29. Denisova, T.G. and Emel'yanova, N.S., *Kinet. Katal.*, 2003, vol. 44, no. 4, p. 485 [*Kinet. Catal.* (Engl. Transl.), vol. 44, no. 4, p. 441].
30. Denisov, E.T., Shestakov, A.F., Denisova, T.G., and Emel'yanova, N.S., *Izv. Akad. Nauk, Ser. Khim.*, 2004, no. 4, p. 693.
31. Khursan, S.L., Semes'ko, D.G., and Safiullin, R.L., *Zh. Fiz. Khim.*, 2006, vol. 80, no. 3, p. 445 [*Russ. J. Phys. Chem.* (Engl. Transl.), vol. 80, no. 3, p. 366].
32. Takhistov, V.V., *Organicheskaya mass-spektrometriya* (Organic Mass Spectrometry), Leningrad: Nauka, 1990.
33. Orlov, Yu.D., Lebedev, Yu.A., and Saifullin, I.Sh., *Termokhimiya organicheskikh svobodnykh radikalov* (Thermochemistry of Organic Free Radicals), Moscow: Nauka, 2001.
34. Mallard, W.G. and Linstrom, P.J., *NIST Chemistry Webbook, NIST Standard Reference Database Number 69*, Gaithersburg, Md.: National Inst. of Standards and Technology, 2000.
35. Wang, X.B., Nicholas, J.B., and Wang, L.S., *J. Phys. Chem. A*, 2000, vol. 104, no. 3, p. 504.
36. Viggiano, A.A., Henchman, M.J., Dale, F., Deakyne, C.A., and Paulson, J.F., *J. Am. Chem. Soc.*, 1992, vol. 114, no. 11, p. 4299.
37. Scott, A.P. and Radom, L., *J. Phys. Chem.*, 1996, vol. 100, no. 41, p. 16 502.
38. Frisch, M.J., Trucks, G.W., Schlegel, H.B., Scuseria, G.E., Robb, M.A., Cheeseman, J.R., Zakrzewski, V.G., Montgomery, J.A., Stratmann, R.E., Burant, J.C., Dapprich, S., Millam, J.M., Daniels, A.D., Kudin, K.N., Strain, M.C., Farkas, O., Tomasi, J., Barone, V., Cossi, M., Cammi, R., Mennucci, B., Pomelli, C., Adamo, C., Clifford, S., Ochterski, J., Petersson, G.A., Ayala, P.Y., Cui, Q., Morokuma, K., Malick, D.K., Rabuck, A.D., Raghavachari, K., Foresman, J.B., Cioslowski, J., Ortiz, J.V., Baboul, A.G., Stefanov, B.B., Liu, G., Liashenko, A., Piskorz, P., Komaromi, I., Gomperts, R., Martin, R.L., Fox, D.J., Keith, T., Al-Laham, M.A., Peng, C.Y., Nanayakkara, A., Gonzalez, C., Challacombe, M., Gill, P.M.W., Johnson, B., Chen, W., Wong, M.W., Andres, J.L., Gonzalez, C., Head-Gordon, M., Replogle, E.S., and Pople, J.A., *GAUSSIAN 98, Revision A.7*, Pittsburgh: Gaussian Inc., 1998.
39. Ayala, P.Y. and Schlegel, H.B., *J. Chem. Phys.*, 1997, vol. 107, no. 2, p. 375.
40. Barone, V. and Cossi, M., *J. Phys. Chem. A*, 1998, vol. 102, no. 11, p. 1995.
41. Reed, A.E., Curtiss, L.A., and Weinhold, F., *Chem. Rev.*, 1988, vol. 88, no. 6, p. 899.
42. Jensen, F., *Introduction to Computational Chemistry*, Chichester: Wiley, 1999, p. 429.